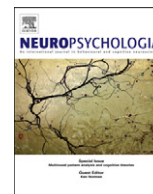




ELSEVIER

Contents lists available at SciVerse ScienceDirect

Neuropsychologia

journal homepage: www.elsevier.com/locate/neuropsychologia

Temporal variability of the N2pc during efficient and inefficient visual search [☆]

Jarrold R. Dowdall ^{a,b,*}, Artur Luczak ^c, Matthew S. Tata ^c

^a The Max Planck Institute for Brain Research, Frankfurt am Main 60528, Germany

^b Ernst Strüngmann Institute (ESI) for Neuroscience in Cooperation with Max Planck Society, Frankfurt am Main, Germany

^c The University of Lethbridge, Lethbridge, Canada, AB T1K 3M4

ARTICLE INFO

Article history:

Received 2 August 2011

Received in revised form

26 May 2012

Accepted 18 June 2012

Available online 26 June 2012

Keywords:

Attention

Visual search

Event related potentials

Theta

N2pc

EEG

ABSTRACT

Efficient and inefficient visual search are characterized by the difference in the time required to find the target. Efficient “popout” search time is relatively unaffected by increases in the number of search items, whereas inefficient “non-popout” search time requires more time increases in duration. Electrophysiological investigations of the neural correlates of visual search have revealed a component of the event-related potential (ERP) known as the N2pc. The N2pc is thought to reflect the orienting of attention to the target during visual search. If the N2pc is more closely associated in time with the moment of target selection than the onset of the search display, it may be predicted that the N2pc would be delayed or more temporally variable during inefficient compared to efficient visual search. In the present study, we contrasted efficient “popout” search with inefficient “non-popout” search to investigate the hypothesis that the N2pc is temporally associated with the moment of search completion, and this would be reflected as a delayed or attenuated N2pc during non-popout search compared to popout. In Experiment 1, we observed a robust N2pc during popout search, but not during non-popout search. However, sorting trials by the N2pc latency recovered the N2pc during non-popout search. In Experiment 2 we replicated this observation and demonstrated that popout and non-popout search reflected differences in the temporal variability of the N2pc latency. Further investigation using time-spectral analysis suggests that evoked posterior–contralateral theta (4–6 Hz) underlies the N2pc during both popout and non-popout search.

© 2012 Elsevier Ltd. All rights reserved.

1. Introduction

The human visual system has developed mechanisms for directing attention to features and objects of interest in complex scenes. The process of finding and selecting a target among a scene of non-target stimuli is called visual search. A substantial body of research in this area has identified and contrasted two modes of visual search: In popout search, the target is selected efficiently by pre-attentive mechanisms, whereas in non-popout search, target selection is believed to be guided by a more complex interaction between stimulus-driven and top-down processes (Treisman & Gelade, 1980; Wolfe, Cave, & Franzel,

[☆] Author's Note: The authors would like to thank Sheena McInnes, Scott Oberg, and Karla Ponjavic-Conte for their assistance with data collection, Andre Bastos for helpful advice on the data analysis, and Craig G. Richter for helpful advice on the statistical analyses. This research was funded by NSERC Canada Discovery Grants to M.S.T and A.L. An AHFMR grant to A.L. Additional support to J.R.D was provided by the International Max Planck Research School (IMPRS) for Neural Circuits (Frankfurt am Main).

* Correspondence to: Ernst Strüngmann Institute (ESI) for Neuroscience in Cooperation with Max Planck Society Deutschordenstraße 46, D-60528 Frankfurt am Main Germany.

E-mail address: Jarrod.dowdall@gmail.com (J.R. Dowdall).

1989). These two search modes are characterized by the time it takes to complete search given an increasing number of search items: Popout search is typically unaffected by such increases in set size, whereas non-popout search time increases with set size. Thus, during non-popout search it appears as though attention is oriented serially through the search display, whereas attention orienting during popout search appears to be mediated by a parallel process. The goal of the present study was to investigate the neural correlates of visual search by contrasting popout and non-popout search. In Experiment 1, we investigated the stimulus-evoked activity as observed in the event-related potential (ERP) of the electroencephalograph (EEG). In Experiment 2, we expanded our analysis to include time-spectral analysis of the EEG.

Substantial understanding of the neural correlates of visual search has been obtained by investigating the visual ERP time-locked to the onset of a search display. This work has revealed a negative deflection in the ERP waveform, known as the N2pc, occurring 200–300 ms post stimulus over posterior scalp, contralateral to the hemifield in which a target singleton appears (i.e., Luck & Hillyard, 1990a; Luck, Fan, & Hillyard, 1993). Non-target singletons may also trigger an N2pc (e.g., Hickey, McDonald & Theeuwes, 2006), but goal-directed task-set probably plays a

key role (e.g., Kiss, Jolicoeur, Dell'acqua, & Eimer, 2008). Thus, the N2pc is thought to reflect orienting of attention to a salient target among distracters (Luck & Hillyard, 1994a, b) and subsequent enhancement of the target features (Mazza, Turatto, & Caramazza, 2009 a, b). It has therefore been used as an index to track the allocation of attention through visual space (Hickey, Di Lollo & McDonald, 2009; Leblanc, Prime, & Jolicoeur, 2008; Woodman & Luck, 1999, for example).

In the present study, the primary goal was to contrast the N2pc evoked during popout search against that of non-popout search. If the N2pc is only evoked by singletons that capture attention in a “bottom-up” manner, then it should only be present during popout search and be absent during non-popout search. However, if the N2pc reflects successful detection of a target, then it should be present on such trials regardless of the type of search engaged. However, considering the serial nature of non-popout search suggests that the moment of target detection is delayed or more variable (i.e., “jittered”) in time, compared to that during popout search. Thus, if the N2pc is evoked relative to the moment of search completion (target detection), rather than the onset of the search display, then the N2pc during non-popout search may appear delayed or attenuated in the ERP (Luck, Heinze, Mangun, & Hillyard, 1990; Luck & Hillyard, 1990a, 1994b).

Although substantial understanding of the neural correlates of visual search has arisen by examining the N2pc ERP component, the oscillatory brain dynamics that underlie the N2pc have gone relatively unexplored. The goal of Experiment 2 was to investigate oscillatory correlates of attentional selection during visual search.

This approach was motivated by a substantial body of recent work giving insight into neural correlates of cognitive function in the oscillatory activity of the brain. For example, several studies have shown theta phase modulation of gamma-band activity (Canolty et al., 2006; Lakatos et al., 2005; Schack, Vath, Petsche, Geissler, & Moller, 2002), during attention tasks (Doesburg, Green, McDonald, & Ward, 2012; Sauseng, Klimesch, Gruber, & Birbaumer, 2008) and visual perception (Demiralp et al., 2007; Doesburg, Green, McDonald, & Ward, 2009). In addition, it has been shown that an endogenous microsaccadic rhythm (~3.3 Hz) modulated gamma-band synchronization (Bosman, Womelsdorf, Desimone, & Fries, 2009). These experimental findings suggest that theta-oscillations have a modulatory role in the brain, by resetting or entraining other oscillations, such as gamma, and may reflect an endogenous “sampling” rhythm of the environment (Bosman et al., 2009; Doesburg et al., 2009). Therefore, we concentrated our time-spectral analysis on lower frequencies.

A secondary goal was to differentiate the functional N2pc from non-lateralized sensory-evoked signals that can be confounded with the N2pc when computed in the canonical way. The N2pc has often been measured and visualized as a difference between ERP waveforms contralateral and ipsilateral to the target (Ansorge, Kiss, & Eimer, 2009; Kiss, Van Velzen, & Eimer, 2008; Jolicoeur, Brisson, & Robitaille, 2008; Robitaille & Jolicoeur, 2006; Telling, Kumar, Meyer, & Humphreys, 2010). Contrasting contralateral and ipsilateral waveforms isolates those correlates of target selection that are strictly lateralized with respect to the target. However, this approach necessarily negates activity that is not lateralized with respect to the target, which might occur if the left and right hemispheres are not functionally symmetric with respect to attention orienting as has been suggested by neuropsychological (Mesulam, 1981; Posner, Walker, Friedrich, & Rafal, 1984) and functional neuroimaging studies (Corbetta, Kincade, Ollinger, McAvoy, & Shulman, 2000; Corbetta, Miezin, Shulman, & Petersen, 1993; Tata & Ward, 2005). We therefore included a homogeneous target-absent display as has been used in some previous studies of visual orienting (e.g., Luck & Hillyard, 1994a, b; Simson, Vaughn, & Ritter, 1977).

2. Materials and methods

2.1. Participants

Thirty-one students from the University of Lethbridge gave informed consent before participating in the experiment. All reported normal or corrected-to-normal vision, and received course credit for their participation. Of these, the data from six participants were excluded due to excessive artifact contamination (i.e., eye movements, blinks, muscle artifact, etc), and twelve participants were excluded because they failed to detect the target on a sufficient number of trials (see below). Therefore, the data from thirteen participants (6 female; 12 right-handed; *mean age* = 23.5 years) were entered into the analysis. The experimental protocol was consistent with the Declaration of Helsinki and was approved by the University of Lethbridge Human Subjects Review Committee.

2.2. Stimuli and procedures

Participants sat 57 cm from the display monitor in a sound-attenuated room under standard fluorescent lighting. The stimuli were presented on a 19 CRT monitor (Dell M992) colour calibrated with Pantone ColorVision Spyder for CRT monitors using OptiCal 3.7.7 software. All stimuli were black on a white background. The refresh rate of the monitor was set to 100 Hz, and display changes were locked to this refresh rate. Stimulus presentation was controlled by custom C/C++ code (which used GL Utilities Toolkit and OpenGL) running on an Apple Mac Mini with an NVIDIA GeForce 9400 graphics card. Participants advanced trials and entered responses via a Bluetooth Macintosh keyboard, and all participants used their right hand regardless of their hand dominance.

Before beginning the experiment participants performed 48 practice trials of each search type. Participants were verbally instructed that the goal of the practice was to become familiar with the task and comfortable making responses. Responses were not collected during the practice, nor was any feedback provided. Speed and accuracy were equally emphasized in the instructions. Both the practice and the experiment were self-paced (i.e., participants initiated each trial), and participants were instructed to take rest breaks as needed.

An experimental block consisted of 96 visual-search trials designed to elicit either popout or non-popout search (Fig. 1A and B). We exploited a well-known asymmetry in visual search (Treisman & Souther, 1985): Circles with a gap “popout” from closed circles, whereas closed circles do not popout among those with a gap. Thus popout search displays contained either a C among Os (target present), or all Os (target absent), and non-popout search displays contained either an O among Cs (target present), or all Cs (target absent). Each participant completed two blocks of each condition (three non-popout set sizes, and four popout set sizes, in a randomized order). Each block began with a screen indicating the target shape for that block. Each trial began with a variable fixation period from 1000 to 2000 ms (rectangularly distributed) during which only the fixation cross was present. The central fixation-cross remained throughout each trial. After fixation the target display appeared for 20 ms, and consisted of two, four or eight search items arranged in a notional circle around fixation. Search items for each set size were arranged such that the display was symmetrical both left/right and top/bottom, and no search items were on the vertical midline. Each search item subtended 3° of visual angle, and was centered 8.5° from fixation. The gap in open circles subtended 1° of visual angle (approximately 1/5 the circumference). The task was to indicate the presence or absence of the target shape by pressing the up arrow or down arrow, respectively. The target was present on half of the trials, and presented at each search item location with equal frequency.

2.3. EEG recording and analysis

The EEG was recorded at 128 scalp sites (Ag/AgCl electrodes, sampled at 500 Hz with a low-pass filter at the Nyquist limit, and referenced to the vertex) with a HydroCel Electrical Geodesics sensor net (Electrical Geodesics Inc., Eugene, OR, USA). Electrode impedances were maintained below 100 kΩ. Offline the EEG was band-pass filtered between 0.3 and 100 Hz (12 dB/octave and 24 dB/octave, respectively; both zero-phase Butterworth filters). The data were analyzed using the BESA software package (BESA GmbH, Gräfelfing, Germany), and MATLAB (MATLAB version 7.12.0; The Mathworks Inc., 2011, Natick, Massachusetts, USA) using the EEGLAB (Delorme & Makeig, 2004) and FieldTrip (Oostenveld, Fries, Mairs, & Schoffelen, 2011) toolboxes. Trials on which an incorrect response was made were excluded from further analysis. Participants were required to successfully detect the target on a minimum of 30 (out of 48) trials within each search type and in each hemifield (right and left). Thus, we reduced the possibility of including confounding data (such as visual acuity differences between visual fields), as well as a hemispheric bias in the EEG purely due to differences in trial number.

Chronically noisy electrodes were identified using the SCADS method (Junghöfer, Elbert, Tucker, & Rockstroh, 2000). All channels were visually inspected before interpolation and a conservative approach was used toward interpolating electrodes (five or fewer per participant). All trials were epoched

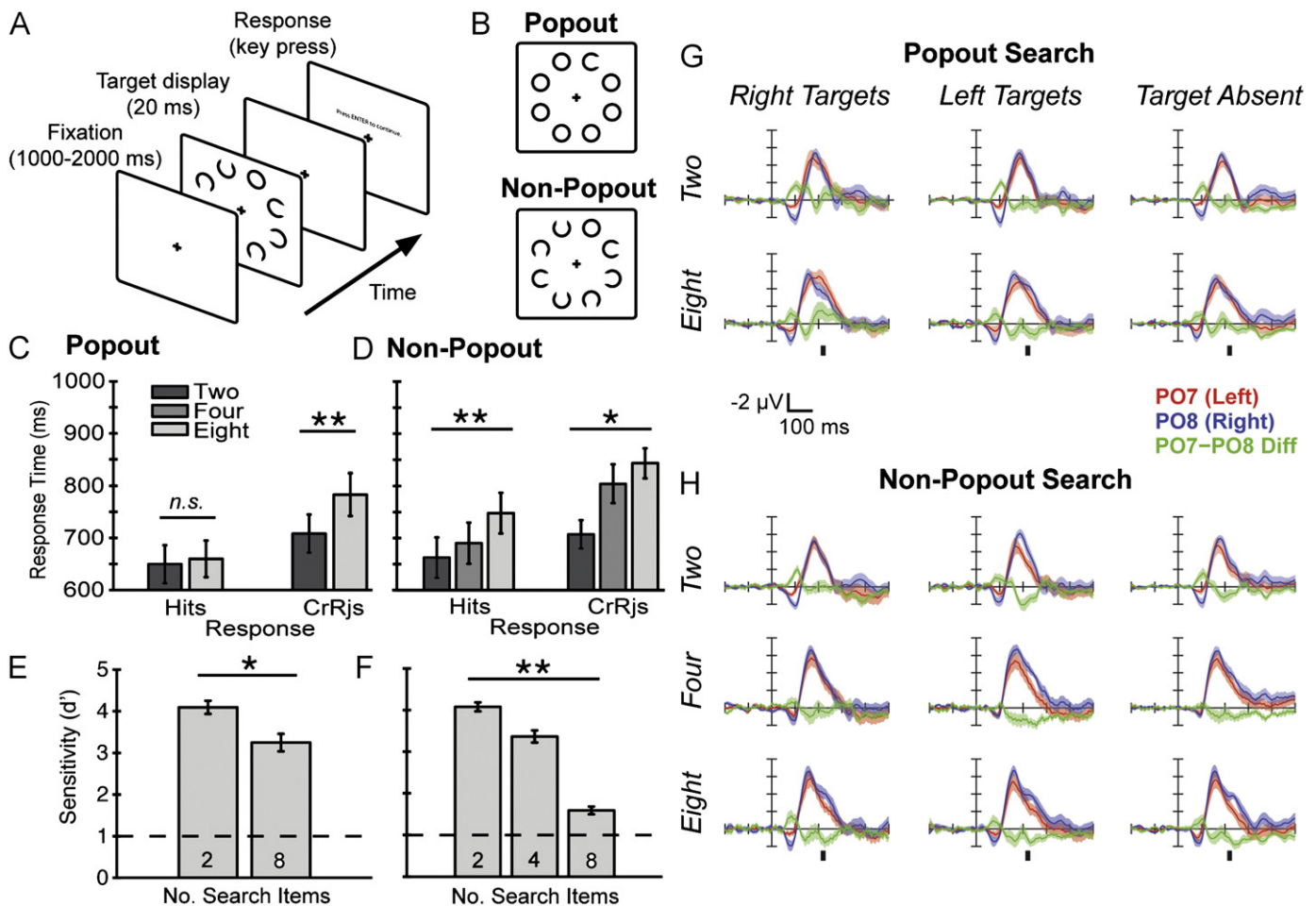


Fig. 1. (A) Design of Experiment 1 showing the trial timeline. Response screen was displayed until response was made. (B) Example eight item (target present) search displays for popout search (parallel), and non-popout search (serial) types. ((C) and (D)) Response times for target present trials (Hits) and target absent trials (Correct Rejections) during popout search and non-popout search, respectively. Note that the 4-item condition was run only for non-popout search. ((E) and (F)) Sensitivity to detect the target for popout search and non-popout search, respectively. (* indicates $p < 0.01$; ** indicates $p < 0.001$). ((G) and (H)) Popout and Non-popout search ERP waveforms (PO7 and PO8) for all set sizes and target conditions including the PO7–PO8 difference waveform. All ERP waveforms are plotted with standard error bars. For eight search items, the window (210–230 ms) over which the N2pc amplitude was computed is indicated with a small bar below the ERPs.

from -200 to 500 ms (-200 to 0 ms baseline), time-locked to the onset of the search display. We used fixed thresholds (amplitude $> \pm 120$ μV ; gradient $> \pm 75$ $\mu\text{V}/\text{ms}$; std. dev. < 0.001 $\mu\text{V}/\text{ms}$) to detect artifact on individual trials, and rejected contaminated trials. Prior to the artifact scan a 60 Hz notch-filter was applied. After interpolation and artifact rejection, we again maintained the same minimum trial criterion as discussed, thus participants with fewer than 30 trials remaining (per condition per target hemifield) were excluded from further analysis. For analysis, the montage was digitally re-referenced to the average reference.

For the purpose of plotting ERP waveforms and ERP statistics, prior to computing the ERPs the EEG was filtered with a low-pass (30 Hz, zero-phase, 24 dB/Octave) Butterworth. All statistical analyses were performed using PASW Statistics 18 (Version 18.0.0, 2009, Chicago, IL), unless otherwise noted. Repeated-Measures Analysis of Variance (ANOVA) was used to test main effects and interactions. We report the p -values based on the Greenhouse–Geisser adjustment for violations of sphericity, however we report the original degrees of freedom for the F ratios. Where appropriate, pairs of means were also compared by paired-samples t -tests, which were two-tailed unless otherwise noted.

2.4. Trial sorting and median split

To investigate the possibility of temporal jitter of the N2pc, we sorted trials by the time at which the maximum contralateral negativity was reached between 200 and 460 ms. The time range between 200 and 460 ms was chosen to be consistent with the time range of the N2pc (200–300 ms). The contralateral negativity was computed for right-hemifield (left-hemifield) targets by subtracting individual trial epochs ipsilateral from contralateral, PO8 from PO7 (PO7 from PO8), and averaging the difference over 20 ms non-overlapping time windows centered from 200 to 460 ms post search display onset. The time of the maximum

contralateral negativity was taken as the center of that time bin. After sorting the trials by these latencies, we split the trials by the median. That is, we used the half of the trials with the earliest N2pc latencies and recomputed the ERP.

3. Results

3.1. Behavioural results

3.1.1. Response time

Participants mean response time (RT) for correctly identifying the presence (hit) and absence (correct rejection) of the target were calculated for both search types and number of search items within each search type (Fig. 1C and D). For each participant, response times greater than three standard deviations were removed before calculating mean response time (five or less rejected per mean RT). Popout-search hit RT was not significantly (two-tail paired t -test) different between two and eight search items [$t_{12} = -1.735$, $p = .108$], however correct rejection RT (target-absent trials) did significantly increase between two and eight search items [$t_{12} = -5.292$; $p < .001$; see Fig. 1C]. Non-popout search hit and correct rejection RT significantly increased with the number of search items [$F_{2,24} = 43.070$, $p < .001$, and $F_{2,24} = 11.343$, $p = .003$, respectively; see Fig. 1D]. We explored the possibility of RT differences between targets presented in either

visual field by repeating the same analysis comparing hit RT between right and left visual fields across the number of search items. We did not observe a main effect of target visual field for popout targets [$F_{1,12}=.165$, $p=.692$], or non-popout targets [$F_{1,12}=.022$, $p=.884$].

3.1.2. Target detection

We used d' as the measure of each participant's sensitivity to detect the target (Fig. 1E and F). When participants scored perfect performance (i.e., hit rate=1.0, or false alarm rate=0.0), hit rate was assigned a value of $(1 - 1/2 \cdot N)$ or false alarm rate was assigned $(1/2 \cdot N)$ (N was the total number of target present, or absent trials).

Both non-popout and popout search d' significantly decreased with the number of search items [$F_{2,24}=152.644$, $p < .001$, and $t_{12}=3.421$, $p=.005$, respectively]. There was no significant difference in d' between popout and non-popout search for two search items [$t_{12}=-.195$, $p=.848$], but there was a significant difference in d' between popout and non-popout search for eight search items [$t_{12}=8.790$; $p < .001$]. However, no participant had a d' below 1.0 in either search condition or set size. We explored the possibility of target detection differences between left- and right-hemifields. To do this we compared the hit rate between targets presented in the left and right-hemifield. We did not observe a significant main effect of target hemifield for either non-popout or popout search [$F_{1,12}=.097$, $p=.761$, and $F_{1,12}=0.0$, $p=1.0$, respectively].

3.1.3. Response bias

It is possible by rejecting participants from the analysis based on a minimum number of trials, that the participants included were biased toward responding "target present". If this were the case, it might suggest that some correct detections were in fact "lucky guesses". It is important to note that the d' results indicate that participants could detect the target in both search conditions (chance $d'=0$). To explore this possibility we calculated the Criterion (C) for each participant. The optimal criterion=0, such that participants maximize hits and minimize false alarms. A criterion shift to the left ($C < 0$) indicates a response bias toward "target present", whereas a criterion shift to the right ($C > 0$) indicates a response bias toward "target absent". We tested whether the criterion for each set size within each search types was different from the optimal criterion of zero (two-tail one-sample t -test).

In popout search, participants' criterion selection was shifted toward responding "target present". This difference was not significant for two search items [$mean=-.112$, $SD=.301$; $t_{12}=-1.344$, $p=.204$], but was significant for eight search items [$mean=-.567$, $SD=.301$; $t_{12}=-5.613$, $p < .001$]. In non-popout search, participants' criterion selection was shifted toward responding "target absent" for two search items [$mean=.077$, $SD=.182$; $t_{12}=1.531$, $p=.152$], and "target present" for both four [$mean=-.110$, $SD=.289$; $t_{12}=-1.344$, $p=.193$] and eight search items [$mean=-.184$, $SD=.338$; $t_{12}=-1.968$, $p=.073$]. However, these differences were not significant.

3.2. Electrophysiological results

We calculated the mean amplitude of the N2 peak (210–230 ms) identified from the difference waveforms between PO7 and PO8 (Fig. 1G and H). Here we focused our comparison between popout and non-popout search for eight search items, however, we present the ERPs from all set sizes with the difference waveforms (PO7–PO8) (Fig. 1G and H).

3.2.1. The N2pc averaged over all trials

Popout search revealed a significant (RANOVA) interaction between target hemifield (left/right/absent) and the recording site (PO7/PO8) reflecting contralaterality of the cortical response to the target [$F_{2,24}=11.344$, $p=.001$; see Fig. 2C]. We also observed a significant main effect of target hemifield [$F_{2,24}=3.823$, $p=.042$], but no main effect of recording site [$F_{1,12}=.023$, $p=.881$]. The N2pc should be reflected as pair of differences between the recording sites (PO7/PO8) for both right and left-side targets, however these differences were not significant [$t_{12}=-1.311$, $p=.214$, and $t_{12}=1.269$, $p=.229$, respectively]. Although, the N2pc comparing contralateral to ipsilateral collapsed over target-hemifield was significant [$t_{12}=-3.146$, $p=.008$; see Fig. 2A].

In the non-popout condition, we did not observe a significant (RANOVA) interaction between target hemifield (left/right/absent) and the recording site (PO7/PO8) [$F_{2,24}=.208$, $p=.74$], nor was there a significant main effect of target hemifield [$F_{2,24}=.023$, $p=.881$; see Fig. 2C]. Similarly, the N2pc comparing contra- to ipsilateral collapsed over target-hemifield did not reach significance [$t_{12}=0.76$, $p=.462$; see Fig. 2A]. However, we did observe a trend to significance for the main effect of recording site [$F_{1,12}=4.32$, $p=.06$]. This effect of recording site appeared as a trend to a greater negativity over the right-hemisphere (PO8) compared to the left (PO7). However, this trend was not significant for target absent search [$t_{12}=-1.981$, $p=.071$].

Note that the N2pc isopotential maps are computed on the waveforms collapsed across both target hemifields (Fig. 2B and E). Therefore, they are artificially bilaterally symmetric (along the sagittal plane), and would fail to reveal hemispheric asymmetries as suggested by the greater negativity over the right-hemisphere recording site (Fig. 2C).

3.2.2. N2pc is recovered by the median split

To investigate the possibility that the N2pc is absent from the ERP due to temporal jitter we sorted trials by time of the maximum contralateral negativity (on target present trials only), and computed the ERP over the median split (described in methods).

In the popout condition, we observed a significant (RANOVA) interaction between target hemifield (left/right) and the recording site (PO7/PO8) [$F_{1,12}=25.242$, $p < .001$; see Fig. 2F]. This effect was observed as a significant difference between contra and ipsilateral ERPs collapsed over target-hemifield [$t_{12}=-5.024$, $p < .001$; see Fig. 2D]. However, the N2pc should be reflected as pair of differences between the recording sites (PO7/PO8) for both right and left-side targets, and here we observed a trend to significance for both [$t_{12}=-1.647$, $p=.125$, and $t_{12}=2.135$, $p=.054$, respectively]. Neither the main effect of target hemifield [$F_{1,12}=.026$, $p=.874$], nor recording site were significant [$F_{1,12}=2.114$, $p=.172$].

In the non-popout condition, we observed a significant (RANOVA) interaction between target hemifield (left/right) and the recording site (PO7/PO8) [$F_{1,12}=29.274$, $p < .001$; see Fig. 2F]. This effect was observed as a significant difference between contra and ipsilateral ERPs collapsed over target-hemifield [$t_{12}=-5.411$, $p < .001$; see Fig. 2D]. Similarly, the N2pc should be reflected as pair of differences between the contra compared to ipsilateral recording site for both right and left-side targets. Here we observed a significant difference for left-targets [$t_{12}=3.222$, $p=.008$], but not right-targets [$t_{12}=-2.031$, $p=.609$]. Neither the main effect of target hemifield [$F_{1,12}=.295$, $p=.597$], nor recording site were significant [$F_{1,12}=1.385$, $p=.262$].

To test the possibility that a reduction in trial number, and not the sorting, had led to this observation we computed the contra and ipsilateral waveforms from a random permutation of half of the trials (not shown in figures). This randomization control did not

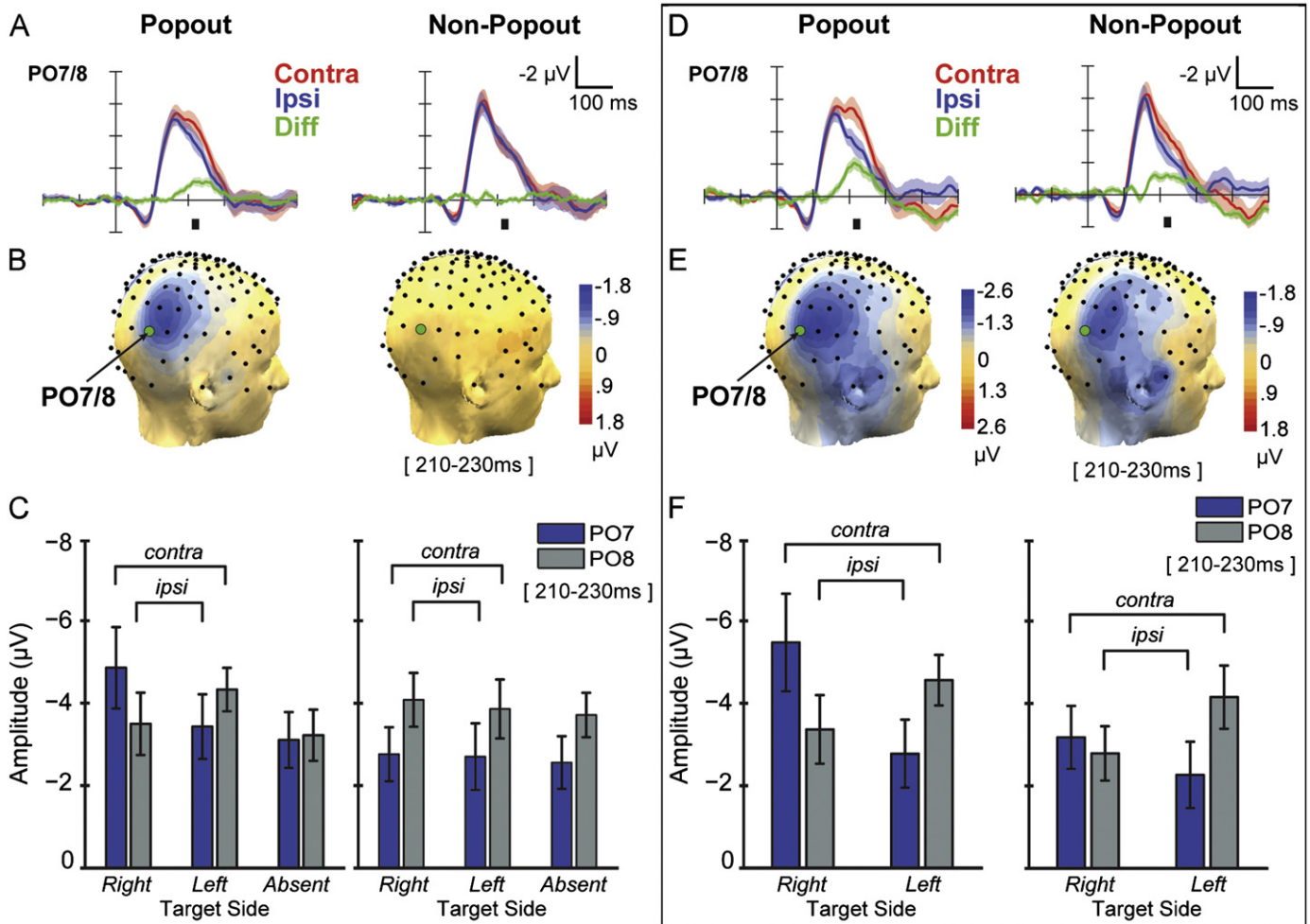


Fig. 2. (A) Experiment 1 ERP contra/ipsilateral (PO7/8) ERP waveforms for both popout and non-popout search computed over all trials. The contra–ipsi difference waveform between contra–ipsi is also plotted. The window (210–230 ms) over which the N2pc amplitude was calculated is indicated with a small bar below the ERPs, and the standard errors bars for each waveform are plotted. (B) Isopotential maps of scalp voltage distribution (210–230 ms) of the contra–ipsilateral difference for both popout and non-popout search with PO7/8 indicated. Note that these plots are bilaterally symmetric (sagittal plane), thus they would fail to reveal hemispheric asymmetries. (C) Bar plots of the N2 amplitude calculated over 210–230 ms (PO7/PO8) for both popout and non-popout search. (D) The contra/ipsilateral (PO7/8) ERP waveforms for both popout and non-popout search computed over the median split of trials sorted by N2pc latency. (E) Isopotential maps of scalp voltage distribution of the N2pc (210–230 ms) for popout and non-popout search computed on the median split, which now shows an N2pc during non-popout search. (F) Bar plots showing the N2pc amplitude computed on the median split. Error bars are the SEM.

reveal a significant N2pc for non-popout search [$mean = -0.093$, $SD = 0.914$; $t_{12} = -.369$, $p = .718$], and the popout N2pc was still significant [$mean = -1.011$, $SD = 1.32$; $t_{12} = -2.763$, $p = .017$].

4. Discussion

Response times for popout and non-popout search were consistent with previous research (Treisman & Souther, 1985). That is, non-popout search response time increased with the number of search items, whereas popout search remained relatively constant. This suggests that popout search reflected efficient “parallel” search and non-popout search inefficient “serial” search, such that the time required to find the target (search completion) increased with the number of search items in non-popout but not popout search.

Here we compared the ERP recorded contralateral and ipsilateral to the target hemifield. This revealed a negative difference at posterior electrodes contralateral to the target hemifield around 220 ms (Fig. 2A and B). This contralateral difference is known as the N2pc, and is thought to reflect target selection in the presence of distractors (Luck et al., 1993; Luck & Hillyard, 1990a, 1994a, b).

We hypothesized that the N2pc would be present when participants detected the presence of the target (hits) regardless of search type.

The N2pc computed over all trials revealed an N2pc for popout but not non-popout search. The absence of an N2pc during non-popout search is of particular interest because the N2pc amplitude has shown to be larger for more difficult-to-find targets (Eimer, 1996; Luck & Hillyard, 1990b; Luck, Girelli, McDermott, & Ford, 1997) and non-targets (Luck & Hillyard, 1994b). One possible explanation is that the N2pc is only evoked by target singletons that direct attention in a “bottom-up” manner. This explanation is consistent with the interpretation of the response time data, such that non-popout targets fail to direct attention efficiently in the visual scene.

However, the response time data also suggest that the moment of search completion (and similarly, target selection) is delayed or more variable in non-popout compared to popout search. Thus, if the N2pc is associated with the moment of target selection, we would predict that the N2pc would be evoked with some temporal variability from trial to trial during non-popout search, but be relatively consistent across trials during popout search. If this theory is true, given a sufficiently large number of

trials, the N2pc during non-popout search would appear to be reduced in amplitude or extended in duration relative to the popout-search condition (Luck et al., 1990; Luck & Hillyard, 1990a, 1994b). The experimental paradigm in this study contained relatively few trials (~30 per target hemifield) compared to what is typical of N2pc studies (100 or more trials). However, we did observe a significant N2pc during popout search, which suggests that it is indeed possible to observe an N2pc with less than the typical number of trials. The fact that the N2pc was observed with this small number of trials in popout but not non-popout search is consistent with the theory that different processes underlie these search modes.

Therefore, we aimed to test the hypothesis that the N2pc was evoked during non-popout search, but rendered invisible in the ERP due to temporal jitter relative to the onset of the search display. By recomputing the N2pc over the median split of trials sorted by N2pc latency, we recovered the N2pc in the non-popout search condition (Fig. 2D and E). This N2pc was observed despite reducing the number of trials in the analysis by 50%, which suggests that the signal-to-noise ratio was increased by rejecting longer-latency N2pc responses from the ERP analysis.

However, it is also possible that the N2pc was not evoked on every trial, such that our sorting method selected those trials that did have an N2pc and discarded those absent of an N2pc. If the N2pc is not evoked on every trial, this would suggest that the N2pc is not necessary for target detection. However, because the paradigm was a two-alternative forced choice task, “lucky guesses” might account for the absence of the N2pc, such that participants correctly “guessed” the target’s presence, but in reality failed to detect the target. The criterion analysis does suggest that participants were slightly biased toward responding

“target present”. Thus, it is possible that participants scored “lucky guesses”, however this effect was more pronounced for popout search rather than non-popout search.

In addition, we observed a right-hemisphere bias in the ERP (210–230 ms). That is, in non-popout search for symmetrical displays (target absent or homogenous condition) electrodes over the right-hemisphere (PO8) compared to the left (PO7) exhibited a larger negative deflection of the ERP (see Fig. 2C). Because the canonical method for computing the N2pc ‘blurs’ any lateralized bias between contralateral and ipsilateral waveforms, the existence of hemispheric asymmetry is a critical point and warrants further investigation.

In Experiment 2 we adapted the method of Experiment 1 to provide more trials for analysis by including only a single set size (eight items). We also reduced the possibility of motor artifact by requiring participants to withhold their response for 1000–1500 ms after the target display onset.

5. Materials and methods

5.1. Participants

Nineteen students from the University of Lethbridge gave informed consent before participating in the experiment. All reported normal or corrected-to-normal vision, and received course credit for their participation. Of these, one participant failed to reach the target detection criterion (see below), and the data from three were excluded due to excessive artifact contamination (i.e., eye movements, blinks, etc.). Therefore, the data from fifteen participants (11 female; 11 right-handed; mean age = 21.7 years) were entered into the analysis. The experimental protocol was consistent with the Declaration of Helsinki and was approved by the University of Lethbridge Human Subjects Review Committee.

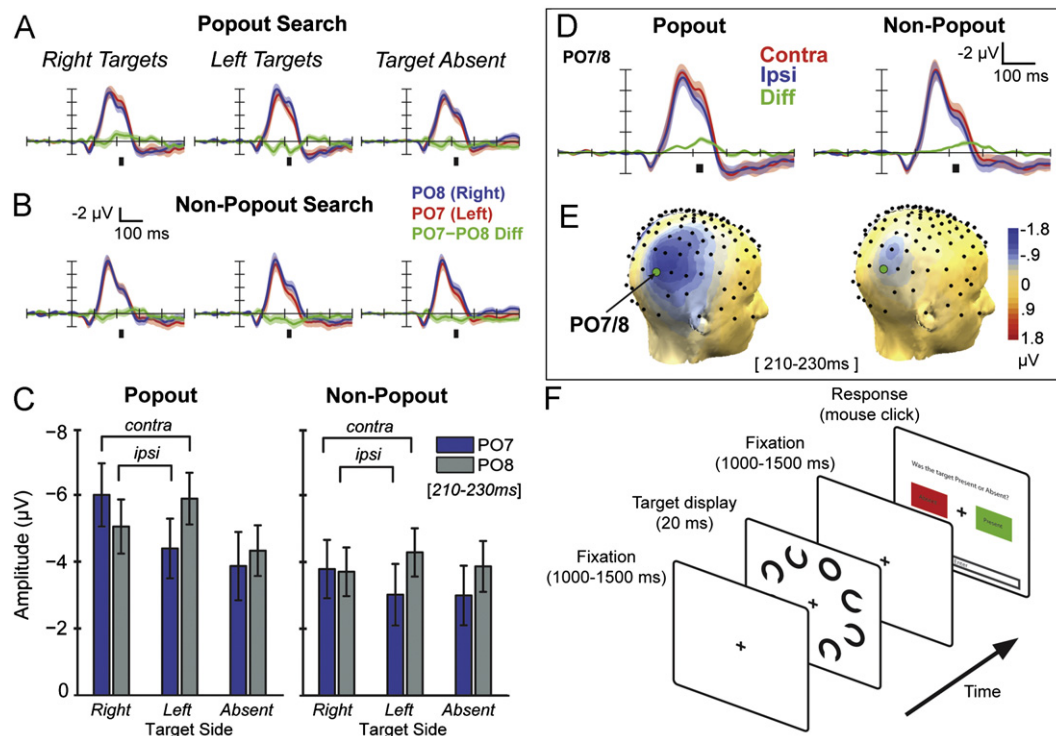


Fig. 3. ((A) and (B)) Popout and Non-popout search ERP waveforms (PO7 and PO8) for all target conditions including the PO7–PO8 difference waveform. All ERP waveforms are plotted with standard error bars. For eight search items, the window (210–230 ms) over which the N2pc amplitude was computed is indicated with a small bar below the ERPs. (C) Mean amplitudes within the N2 latency window for popout and non-popout displays, respectively. Greater contralateral amplitude is evident in popout case, whereas a right-hemisphere bias predominates in the non-popout case. (D) The N2pc computed in the more typical way by collapsing across electrode site to directly contrast ipsilateral with contralateral deflections, for popout and non-popout displays respectively. (E) Isopotential maps of scalp voltage distribution (210–230 ms) of the contra–ipsilateral difference for both popout and non-popout search with PO7/8 indicated. (F) Design of Experiment 2. Participants performed popout or non-popout search as in Experiment 1 except that responses were withheld for a 1000–1500 ms fixation period.

5.2. Stimuli and procedures

The experimental setup was exactly the same as in Experiment 1, however the task was slightly modified (Fig. 3F). In Experiment 2 both conditions always had eight search items, and consisted of eight blocks of trials (four non-popout and four popout in random order). Consistent with Experiment 1, the target was present on 50% of the trials and absent on 50%. Each trial began with 1000–1500 ms of fixation (rectangularly distributed) in which only the fixation cross was visible. The target display then appeared for 20 ms followed by another 1000–1500 ms fixation screen (also rectangularly distributed) during which participants withheld their response. After the post-target fixation a response screen appeared with two boxes allowing participants to select whether the target was present or absent using a Macintosh Bluetooth mouse. The selection boxes were centered 8.5° from fixation (one on the left and the other on the right horizontal midline). The target present box contained the word “Present” and was coloured green, similarly the target absent box contained the word “Absent” and was coloured red. The hemifield in which each selection box was positioned was randomized across trials. As in Experiment 1, participants self initiated trials, and used their right hand regardless of their hand dominance.

5.3. EEG recording and analysis

EEG recording, preprocessing, and analysis methods were as in Experiment 1. The minimum trial criterion was 50 trials (of a possible 80) per search type, per target hemifield. Note, that this criterion is related to that in Experiment 1 (i.e., min. trials $\geq 62.5\%$ of total).

5.3.1. Sorting trials by maximum N2pc

In Experiment 2, we employed the same maximum contralateral negativity sorting method as applied in Experiment 1. However, because we had more trials and aimed to further test the N2pc temporal jitter hypothesis, we split the sorted trials into five non-overlapping bins containing ten trials each. Thus, in this analysis, we excluded the trials with the latest maximum contralateral negativity when a participant had more than 50 trials (per target hemifield). This trial cut-off was chosen because the minimum trial criterion in this Experiment was 50 trials, thus all participants had a minimum of 50 trials. In addition, this cut-off ensured that the number of trials was held constant across conditions and participants.

To investigate the temporal variability of the N2pc, we computed the ERP across the ten trials in each bin and determined the maximum contralateral negativity (difference between contralateral and ipsilateral ERPs) between 180 and 490 ms. Thus, for right-hemifield (left-hemifield) targets the ERP at PO8 was subtracted from PO7 (PO7 from PO8). The amplitude of the N2pc (contralateral negative difference) was calculated as the mean over a 20 ms window centered on the peak maximum, and the time point of the peak maximum was recorded for each of the five trial bins. Thus, the time of the maximum contralateral negativity could range between 180 and 490 ms with the precision of the EEG sampling rate (500 Hz = 2 ms).

5.4. Time-spectral analysis

As previously discussed, the raw EEG was filtered with (high-pass: 0.3 Hz and low-pass: 100 Hz) Butterworth filters, and epoched from –1000 to 1000 ms time-locked to target display onset. We computed the discrete Fourier transform (DFT) as implemented in the EEGLAB function *timefreq()* with MATLAB (MATLAB version 7.12.0; The Mathworks Inc., 2011, Natick, Massachusetts, USA). More explicitly, the FFT was applied to the EEG after applying a Hanning taper over 128 samples (256 ms) and zero-padding to 256 samples. The FFT was repeated from –200 to 500 ms in steps of 20 ms. To ensure at least one cycle of each frequency was in the original data, we retrieved the DFT starting at the Rayleigh frequency of our original sample size (256 ms) 3.9 Hz. Zero-padding doubled the frequency resolution (1.95 Hz), and because we focused on lower frequencies we discarded the DFT > 30 Hz. Thus, the time-spectral data was explored between 3.9 and 29.3 Hz in 1.95 Hz steps, and from –200 to 500 ms in 20 ms steps.

The total amplitude change relative to baseline (often referred to as Time Spectral Evolution (TSE)) was computed by dividing amplitude by the mean baseline amplitude (–200 to 0 ms) for each frequency over the whole epoch (–200 to 500 ms) and multiplying by 100. We then computed the combined contralateral and ipsilateral (PO7/PO8) TSEs by averaging over target hemifield (left and right targets) for each participant. Finally, the difference between contralateral and ipsilateral TSEs was computed, and the grand average computed over participants.

The evoked theta amplitude was calculated by averaging the DFT (i.e., complex values) over trials, which is equivalent to first averaging the EEG over trials and then transforming the ERP into time-frequency space, and then dividing by the mean baseline evoked amplitude (–200 to 0 ms). Similar to TSE, we then computed the combined contralateral and ipsilateral (PO7/PO8) evoked amplitude by averaging over target hemifield (right and left targets) for each participant, and

the grand mean difference was computed over participants. To isolate the theta band activity, we averaged over the frequency bins from 4 to 6 Hz.

Similar to the ERP analysis, we sorted and binned the DFT and computed the Evoked Theta Amplitude for each bin. Importantly, we sorted the DFT trials by the latency of the N2pc ERP component, and only included the first 50 trials with the earliest N2pc ERP latency in the analysis. However, to reduce noise, we computed the Evoked Theta for each bin over 20 trials, of which 15 trials overlapped between adjacent bins. Thus, this resulted in seven bins of 20 trials sorted by N2pc ERP latency with 75% trial overlap. We then computed the Spearman's rank correlation coefficient across sorted bins for both search conditions. To test the significance of the correlation coefficients we employed permutation statistics.

5.4.1. Permutation statistics

We employed non-parametric permutation statistics at the second level to test for significant time-spectral differences over participants. That is, the permutation was performed between the values of interest averaged over trials for each participant. Thus, no permutations were done at the single trial level.

To test for significant differences between contralateral relative to ipsilateral TSE, we permuted the assignment of contralateral and ipsilateral within each participant, and recomputed the grand mean difference to build a surrogate distribution. We computed all possible combinations ($N^k - 1$ combinations, where N is the number of conditions and k the number of participants) for the surrogate distribution. To control for multiple comparisons over many time/frequency bins, we took the maximum and minimum value over all time/frequency bins for each permutation, and entered those values into the surrogate distribution. Lastly, the surrogate distribution of max and min values were sorted and the max value $> 97.5\%$ of the permuted max values, and the min value $< 97.5\%$ of the permuted min values were taken as the threshold for significance.

To test for significance of the Spearman's rank correlation coefficient across sorted bins, the evoked theta amplitude for each bin was randomly reordered for each participant, and the grand mean difference over participants recomputed for each bin. Then the latency of the maximum contralateral evoked theta amplitude was determined for each bin on the grand mean difference. Importantly, the N2pc ERP bins were never permuted, and thus maintained the same sorted order throughout. The Spearman's correlation coefficient was computed across bins on the latency values for the permuted evoked theta amplitude and the sorted N2pc ERP latency. This R value entered the surrogate distribution, and the process repeated 50,000 times. We calculated a two-tail p value for the original R value by determining the proportion of surrogate R values greater than or equal to the original R value and multiplying this proportion by two.

6. Results

6.1. Behavioural results

In Experiment 2, participants withheld their response for 1000–1500 ms post-target display therefore there are no response times to report. The sensitivity to detect the target (d') was calculated as in Experiment 1. We found popout search d' [$mean=3.92$, $SD=.77$] was significantly greater than non-popout d' [$mean=2.22$, $SD=.60$; $F_{1,14}=8.339$, $p < .001$]. To explore the possibility of target detection differences between visual field we compared right and left hit rate using a two-tail paired samples t -test. We did not find a significant difference between target visual field (right vs. left hit-rate) in popout search [$t_{14}=0.0$, $p=1.0$], however this difference was significant for non-popout search [$t_{14}=2.732$, $p=.016$]. The mean hit rate for right-hemifield targets was [$mean=.8967$, $SD=.0836$], and left-targets was [$mean=.8307$, $SD=.0707$; $mean$ trial number difference = 5.5, $SD=7.5$]. Thus participants were slightly better at detecting non-popout targets when presented in the right compared to left-hemifield.

As in Experiment 1, we calculated the Criterion (C) for each participant and compared the result to zero using a one-sample t -test (two-tail). As in Experiment 1, for popout search participants' criterion selection was shifted toward responding “target present” [$mean=-0.45$, $SD=.352$, $t_{14}=-4.949$, $p < .001$], whereas for non-popout search participants appeared to select the optimal criterion that maximizes hits and minimizes false alarms [$mean=-0.027$, $SD=.3805$, $t_{14}=-.278$, $p=.785$].

6.2. Electrophysiological results

6.2.1. The N2pc averaged over all trials

As in Experiment 1, for popout search, we observed a significant (RANOVA) interaction between target hemifield (left/right/absent) and the recording site (PO7/PO8) reflecting contralaterality of the cortical response to the target [$F_{2,28}=18.632, p < .001$; see Fig. 3A and C]. We also observed a significant main effect of target hemifield [$F_{2,28}=25.392, p < .001$], but no main effect of recording site [$F_{1,14}=.369, p=.553$]. Here we also aimed to test that the N2pc would be reflected as pair of differences between the recording sites (PO7/PO8) for both right and left-side targets. We observed a significant difference for left-hemifield targets [$t_{14}=2.404, p=.031$], and a trend to significance for right-hemifield targets [$t_{14}=-1.733, p=.105$]. As in Experiment 1, the N2pc comparing contralateral to ipsilateral when averaged over target-hemifield was significant [$t_{14}=-5.645, p < .001$, see Fig. 3D].

In the non-popout condition, contrary to Experiment 1, we observed a significant (RANOVA) interaction between target hemifield (left/right/absent) and the recording site (PO7/PO8) [$F_{2,28}=16.568, p < .001$; see Fig. 3B and C]. However, the main effect of target hemifield was not significant [$F_{2,28}=1.539, p=.232$]. Similar to popout search, we observed a significant difference between PO7/PO8 for left-hemifield targets [$t_{14}=2.42, p=.042$], but failed to observe a significance difference for right-hemifield targets [$t_{14}=-.157, p=.878$]. However, the N2pc comparing contralateral to ipsilateral when averaged over target-hemifield did reach significance [$t_{14}=-4.446, p=.001$; see Fig. 3D]. Therefore, this suggests that the N2pc effect here is dominated by a difference between PO7 and PO8 for left-hemifield targets.

Although, we did not observe a significant main effect of recording site [$F_{1,14}=1.843, p=.196$], similar to Experiment 1, we observed a trend to significance comparing PO8 to PO7 for the target absent condition [$t_{14}=-1.820, p=.090$].

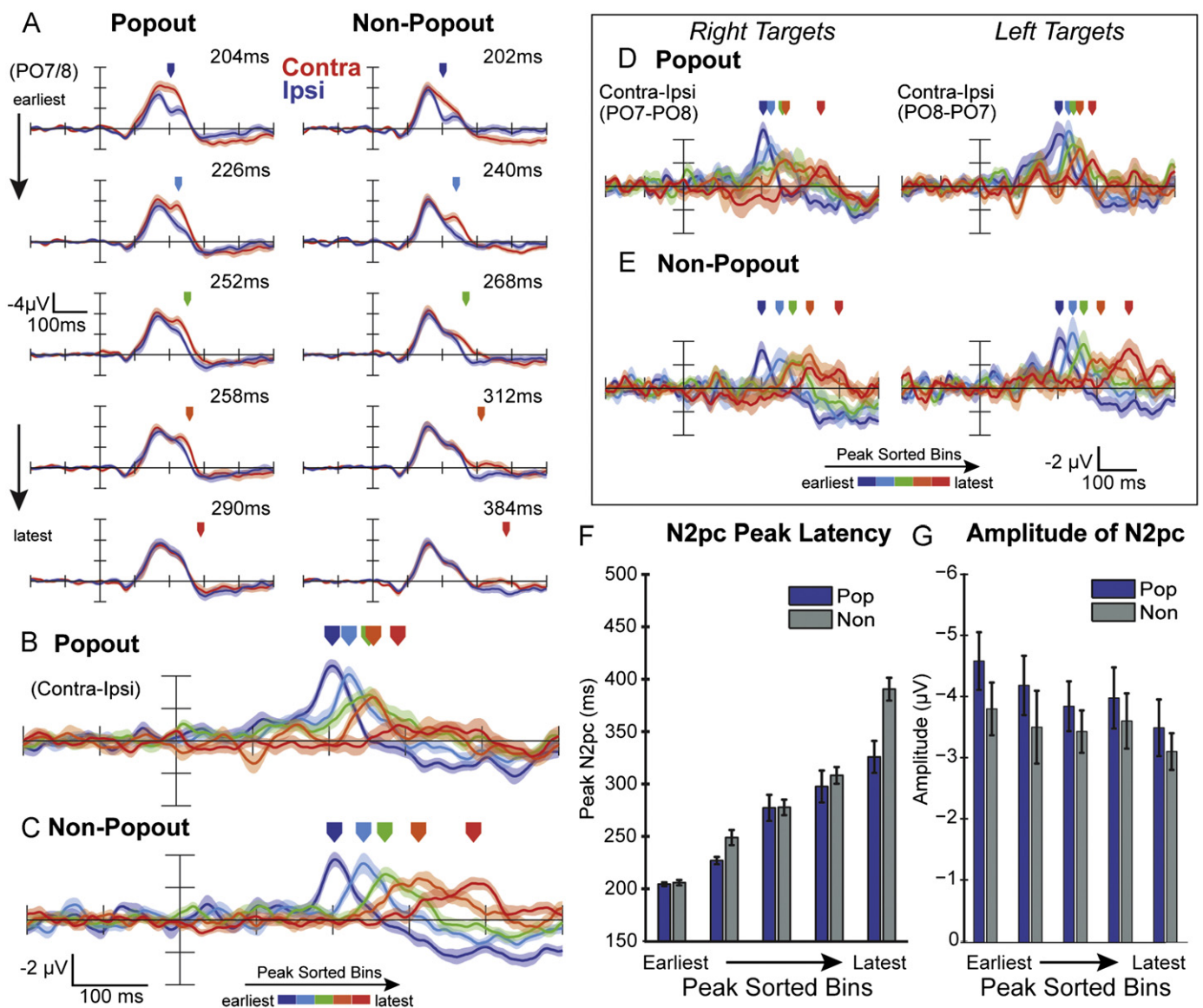


Fig. 4. (A) The contra/ipsilateral ERP waveforms computed for each sorting bin collapsed over target hemifield (PO7/8). The peak of the difference waveform is indicated above. (B) Popout search N2pc contra-ipsi difference waveforms. The peak of N2pc is indicated for each sorting bin. (C) Non-popout search N2pc contra-ipsi difference waveforms. The peak of N2pc is indicated in for each sorting bin. (D) Popout differences waveforms for both left and right targets. (E) Non-popout differences waveforms for both left and right targets. (F) Bar plot showing the mean and SEM N2pc peak latency over participants for each sorting bin for popout and non-popout search. Computed on the collapsed contra-ipsilateral difference waveform (PO7/8). (G) Bar plot showing the mean and SEM N2pc peak amplitude over participants for each sorting bin for popout and non-popout search. Computed on the collapsed contra-ipsilateral difference waveform (PO7/8).

6.2.2. *N2pc sorted*

To further test the jittered N2pc hypothesis, similar to Experiment 1, we sorted the individual trials by the time of the maximum contralateral negativity (between 200 and 460 ms). However, because there were more trials in Experiment 2 we binned the

earliest 50 trials into five (non-overlapping) bins of ten trials each, and computed the ERP for each bin (described in methods).

We tested whether there was a significant difference between contralateral and ipsilateral waveforms within each latency bin (collapsed over target hemifield) using paired *t*-tests (see Fig. 4A).

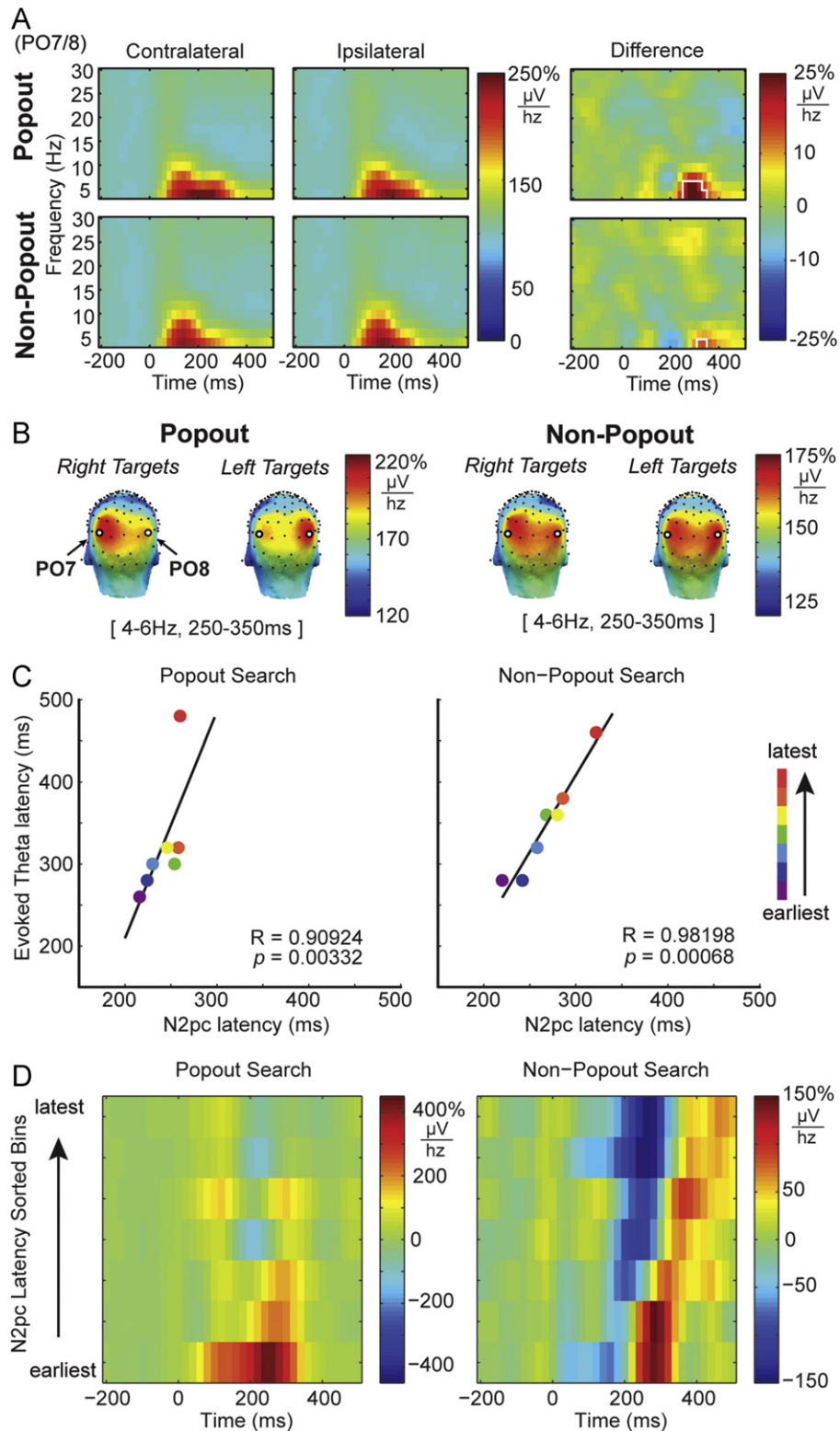


Fig. 5. (A) Total amplitude relative to baseline for both popout and non-popout search. Contra–ipsi difference is plotted in the right column. (B) The topographical representation of the total theta (4–6 Hz) amplitude for left and right targets (averaged from 250–350 ms). (C) Correlation plot between N2pc latency and the latency of evoked theta. Plots show the linear least-squares line for both search types (black). (D) The contra–ipsilateral (PO7/8) difference for evoked theta amplitude for each N2pc latency sorted bin.

The peak time was determined from the difference waveform in each bin separately, and the mean computed over a 20 ms window centered on the peak maximum. The Bonferroni corrected critical p -value in this case was $p < .01$. In popout search, all but the latest latency sorted bin showed a significant difference between ipsi- and contralateral waveforms [$t_{14} = -10.064$, $p < .001$; $t_{14} = -7.508$, $p < .001$; $t_{14} = -5.428$, $p < .001$; $t_{14} = -4.859$, $p < .001$; $t_{14} = -1.599$, $p = 0.132$; earliest to latest, respectively]. In non-popout search, all latency sorted bins showed a significant difference between ipsi- and contralateral waveforms [$t_{14} = -7.493$, $p < .001$; $t_{14} = -5.354$, $p < .001$; $t_{14} = -6.102$, $p < .001$; $t_{14} = -5.922$, $p < .001$; $t_{14} = -5.550$, $p < .001$; earliest to latest, respectively].

To test whether the N2pc latency or amplitude differed across sorted bins, we determined the peak N2pc latency separately for each participant's contra-ipsilateral difference ERP waveform between 180 and 490 ms post-stimulus, and calculated the amplitude over a 20 ms window centered on the peak (describe in methods). With respect to N2pc latency, we observed a significant (RANOVA) interaction between search type (popout/non-popout) and latency bin [$F_{4,56} = 4.296$, $p = .013$; see Fig. 4F], and significant main effects of search type [$F_{1,14} = 5.086$, $p = .041$], and latency bin [$F_{4,56} = 131.732$, $p < .001$]. These results suggest that the latency bins captured systematically different N2pc peak latencies, and that these latencies were different between popout and non-popout search types.

Although the amplitude of the N2pc appears to decrease with peak latency, we did not observe a significant (RANOVA) interaction between search type (popout/non-popout) and latency bin [$F_{4,56} = .208$, $p = .903$; see Fig. 4G], or a significant main effect of latency bin [$F_{4,56} = 1.539$, $p = .226$]. However, the main effect of search type tended to significance [$F_{1,14} = 4.494$, $p = .052$]. These results suggest that the amplitude of the N2pc was not significantly different over the latency bins, but that the amplitude tended to be different between popout and non-popout search types.

6.3. Time-spectral results

The time-spectral analysis was designed to isolate the oscillatory activity contralateral to the target (i.e., the N2pc). Thus, we compared the time-spectral representation of EEG data contralateral to the target relative to ipsilateral (Fig. 5).

6.3.1. Total amplitude relative to baseline

We isolated the oscillatory activity related to the N2pc by comparing contralateral to ipsilateral time-spectral representations at PO7/PO8. The *total amplitude*, or Time-Spectral Evolution (TSE), is sensitive to both evoked (phase-locked) and induced (non-phase-locked activity). Thus, comparing the TSE contralateral to ipsilateral should reveal any differences regardless of the phase relation relative to stimulus onset across trials.

We computed the TSE over all trials for each participant, for each target hemifield, and collapsed over hemifield by averaging the contralateral and ipsilateral channels with respect to the target hemifield (Fig. 5A). We used non-parametric permutation statistics to test the significance of the TSE difference over contralateral and ipsilateral cortices, and used the max/min threshold to correct for multiple comparisons across multiple time/frequency bins (described in methods). This analysis (Fig. 5) revealed significantly greater contralateral TSE for both popout search (4–6 Hz; 250–350 ms), and non-popout search (4 Hz; 320–350 ms).

6.3.2. Evoked theta amplitude

Evoked oscillatory activity is the component of EEG signal that is phase-locked to an event of interest. It is this portion of the EEG that is captured by the ERP waveform. Here we directed our analysis given the previous results of TSE amplitude showing that Theta (4–6 Hz) was significantly greater contralateral to the target hemifield in both search conditions. Similar to the ERP analysis, we sorted and binned the DFT and computed the Evoked Theta Amplitude for each bin. Importantly, we sorted the DFT trials by the latency of the N2pc ERP component, and only included the first 50 trials with the earliest N2pc ERP latency in the analysis. However, to reduce noise, we computed the Evoked Theta for each bin over 20 trials, of which 15 trials overlapped between adjacent bins. Thus, this resulted in seven bins of 20 trials sorted by N2pc ERP latency with 75% trial overlap (Fig. 5D).

The latency of the N2pc component was determined by taking the time point of the maximum contralateral negativity of the grand average difference for each bin (180 and 480 ms, with a sliding average of 20 ms). The latency of the maximum contralateral evoked theta amplitude (between 180 and 480 ms) was also determined for each bin. We then computed the Spearman's rank correlation coefficient between N2pc and evoked theta peak latencies across sorted bins for both search conditions (Fig. 5C). To test the significance of the correlation coefficients, we employed non-parametric permutation statistics (described in methods). The Spearman's rank correlation coefficient across sorted bins showed a positive relationship and was significant for both popout [$R = 0.9092$; $p = 0.00332$], and non-popout search [$R = 0.9820$; $p = 0.00068$].

7. Discussion

In Experiment 1 we tested the hypothesis that the N2pc evoked during both popout and non-popout search, but is temporally jittered during non-popout search thus rendering it invisible in the ERP. Sorting trials by the latency of the peak N2pc, and recomputing the ERP waveforms on the median split revealed a significant N2pc during non-popout search. However, another possible explanation for this result is that the N2pc was not present on every trial. Therefore, Experiment 2 was designed to further test the jittered N2pc hypothesis with more trials for the analysis.

Experiment 2 closely replicated Experiment 1. As in Experiment 1, we observed a significant contralateral negative deflection of the ERP waveform at the N2 latency in popout search, however we also observed a significant N2pc in non-popout search (collapsed over target hemifield). The observation that simply more trials revealed an N2pc in non-popout search is consistent with the hypothesis that N2pc is indeed jittered. However, it should be noted that this contralateral difference during non-popout search was dominated by a contralateral difference for left-hemifield targets, but not right-targets. Thus, it could be argued that this is not an N2pc as classically defined, and underscores the importance of comparing contralateral to ipsilateral within target hemifield before collapsing across target hemifields.

As in Experiment 1 we sorted trials by the latency of the N2pc component, but here we aimed to test the jittered N2pc hypothesis with better temporal resolution. Importantly, we specifically aimed to test the hypothesis that the N2pc during non-popout search was evoked with more temporal variability compared to popout search. Thus, we binned the sorted trials into five bins, and computed the canonical N2pc ERP waveforms. This analysis revealed a temporally jittered N2pc in both popout and

non-popout search, which also appeared evoked at longer latencies during non-popout search. To systematically test that the N2pc was evoked at longer latencies in non-popout compared to popout search we determined the peak latency in each sorted bin for each participant. This analysis revealed a consistent difference in N2pc latency between non-popout and popout search. Secondary to the latency analysis, it appeared as though the amplitude of the N2pc decreased with latency, thus we also compared the amplitude across participants. This analysis revealed only a minimal effect of decreasing amplitude over latencies, however, more significant was a consistent amplitude difference between popout and non-popout search.

An additional aim of Experiment 2 was to investigate the oscillatory dynamics of the N2pc. This analysis revealed that evoked theta (4–6 Hz) latency correlation with the latency of the N2pc.

As in Experiment 1, we observed a small but reliable tendency for the right-side recording site (PO8) to exhibit a larger negative difference relative to the left (PO7), particularly during non-popout search. Importantly, this signal was obscured in the canonical contra- versus ipsilateral analysis of the N2pc component. Its existence is consistent with observations that right-hemisphere is involved in spatial orienting processes. Hemispheric asymmetries have been reported before in N2pc literature. For example, Eimer (1996) reported a left-hemispheric bias for target words presented in the right-hemifield. It is known that the left-hemisphere is specialized for language processing. Thus, it certainly interesting to speculate that the absence of an N2pc over one hemisphere might be due to latency differences between the hemispheres in orienting to specific types of target stimuli.

8. Conclusion

In two experiments we contrasted the neural mechanisms of efficient and inefficient visual search. In Experiment 1, we showed that the N2pc ERP component is evident during efficient popout search, but not during inefficient serial search. However, a median split of the trials sorted by the latency of the N2pc recovered an N2pc component for non-popout search, consistent with the notion that inefficient search displays lead to temporally variable N2pc events.

Experiment 2 was designed to maximize the number of trials available for both time-frequency analysis and investigation of the trial-to-trial latency of the N2pc. Employing the same sorting method as in Experiment 1, but with multiple sorted bins, revealed an N2pc that occurred later and later in time. Importantly, the N2pc latency range during non-popout search was extended in duration compared to popout search. Finally, we show that evoked theta-band activity reflects the N2pc for both search types.

8.1. Efficient vs. inefficient search: Temporal jitter of N2pc

In both Experiments 1 and 2, we observed that sorting individual trials into bins according to the latency of the maximum negative deflection within the N2pc window yielded a larger N2pc, or recovered the N2pc that was invisible in the grand average ERP (averaged over all trials). What is important here is the difference in the latency range over which the N2pc appears in popout compared to non-popout trials: The N2pc during popout search fell within a relatively narrow range of 86 ms between the N2pc in earliest and latest bin. By contrast, non-popout N2pc latencies ranged over 182 ms. Importantly, the earliest latency bins in the two conditions fell within two milliseconds, suggesting that on some trials the popout and non-popout N2pc occurred at a similar latency.

One possible interpretation is that the N2pc is an ERP component that is time locked to a cognitive event (target selection) rather than a stimulus event (display onset). That is, the N2pc is time locked to display onset only insofar as target selection is time locked to display onset. The formation of an ERP waveform from EEG data requires sharp time-locking of brain responses to the events that triggered them. Therefore, jitter in the time-locking of the N2pc relative to display onset would therefore be expected to reduce its amplitude.

The question remains whether the N2pc latency correlates with response time (RT). Seemingly inconsistent with the observations reported here, Mazza et al. (2009a) reported a larger N2pc amplitude for search displays with more search items. However, RTs were significantly faster for search displays with more search items. Additionally, they report a temporally delayed N2pc for search displays with heterogeneous compared to homogenous distractors, of which RTs to heterogeneous displays were significantly slower. In a similar study, Mazza et al. (2009b) reported an earlier N2pc when features of the target were constant across trials as opposed to variable, and again RTs were slower for the variable target condition. However, they also report a larger N2pc when participants were required to discriminate the target compared to simply detect the presence of the target, and RTs were significantly slower for target discrimination task. These results suggest that relationship between N2pc latency or amplitude may depend on the task type.

Here we have not correlated response times on individual trials with the latency of the N2pc. In Experiment 2, response time analysis was not possible because participants withheld their response for a variable delay period, which was done to reduce the possibility of motor artifact in the post-stimulus period. In Experiment 1, we did analyze ERPs locked to response times (data not shown) however these waveforms were substantially distorted, most likely due to the temporal jitter of the response times, and the results were difficult to interpret.

8.2. The N2pc and evoked theta

An additional aim of Experiment 2 was to explore the oscillatory dynamics of the N2pc. This analysis revealed a contralateral component in the theta-band (4–6 Hz) evident in the total amplitude relative to baseline. We further tested the relationship between theta and the N2pc by analyzing evoked theta amplitude and correlating the latency of the N2pc with the latency of the contra-ipsilateral evoked theta difference. This analysis suggested that the N2pc is related directly to evoked theta. That is, theta-band activity with phase consistency across trials. Furthermore, these results are consistent with the jittered N2pc hypothesis, such that the evoked theta latency range was extended in duration for non-popout compared to popout search.

The analysis here suggests that theta-band oscillations become phase-locked relative to the moment of target selection. However, the functional significance of such theta-band synchronization remains speculative. Several studies have shown theta phase modulation of gamma-band activity (Canolty et al., 2006; Demiralp et al., 2007; Doesburg et al., 2009, 2012; Lakatos et al., 2005; Sauseng et al., 2008; Schack et al., 2002). Although we did not investigate the relationship between theta and other frequencies here, it is worth speculating that theta phase-synchronization at the moment of target selection may be associated with activity at other frequency bands that may also reflect target-specific processing.

References

- Anson, U., Kiss, M., & Eimer, M. (2009). Goal-driven attentional capture by invisible colors: evidence from event-related potentials. *Psychonomic Bulletin Review*, 16(4), 648–653.
- Bosman, C. A., Womelsdorf, T., Desimone, R., & Fries, P. (2009). A microsaccadic rhythm modulates gamma-band synchronization and behavior. *The Journal of Neuroscience*, 29(30), 9471–9480.
- Canolty, R. T., Edwards, E., Dalal, S. S., Soltani, M., Nagarajan, S. S., Kirsch, H. E., Berger, M. S., Barbaro, N. M., & Knight, R. T. (2006). High gamma power is phase-locked to theta oscillations in human neocortex. *Science*, 313(5793), 1626–1628.
- Corbetta, M., Kincade, J. M., Ollinger, J. M., McAvoy, M. P., & Shulman, G. L. (2000). Voluntary orienting is dissociated from target detection in human posterior parietal cortex. *Nature Neuroscience*, 3(3), 292–297.
- Corbetta, M., Miezin, F. M., Shulman, G. L., & Petersen, S. E. (1993). A PET study of visuospatial attention. *Journal of Neuroscience*, 13(3), 1202–1226.
- Delorme, A., & Makeig, S. (2004). EEGLAB: an open source toolbox for analysis of single-trial EEG dynamics. *Journal of Neuroscience Methods*, 134, 9–21.
- Demiralp, T., Bayraktaroglu, Z., Lenz, D., Junge, S., Busch, N. A., Maess, B., Ergen, M., & Herrmann, C. S. (2007). Gamma amplitudes are coupled to theta phase in human EEG during visual perception. *International Journal of Psychophysiology*, 64, 24–30.
- Doesburg, S. M., Green, J. J., McDonald, J. J., & Ward, L. M. (2009). Rhythms of consciousness: binocular rivalry reveals large-scale oscillatory network dynamics mediating visual perception. *PLoS ONE*, 4(7), e6142.
- Doesburg, S. M., Green, J. J., McDonald, J. J., & Ward, L. M. (2012). Theta modulation of inter-regional gamma synchronization during auditory attention control. *Brain Research*, 1431, 77–85.
- Eimer, M. (1996). The N2pc component as an indicator of attentional selectivity. *Electroencephalography and Clinical Neurophysiology*, 99, 225–234.
- Hickey, C., Di Lollo, V., & McDonald, J. J. (2009). Electrophysiological indices of target and distractor processing in visual search. *Journal of Cognitive Neuroscience*, 21(4), 760–775.
- Hickey, C., McDonald, J. J., & Theeuwes, J. (2006). Electrophysiological evidence of the capture of visual attention. *Journal of Cognitive Neuroscience*, 18(4), 604–613.
- Jolicoeur, P., Brisson, B., & Robitaille, N. (2008). Dissociation of the n2pc and sustained posterior contralateral negativity in a choice response task. *Brain Research*, 1215, 160–172.
- Junghöfer, M., Elbert, T., Tucker, D. M., & Rockstroh, B. (2000). Statistical control of artifacts in dense array EEG/MEG studies. *Psychophysiology*, 37, 523–532.
- Kiss, M., Jolicoeur, P., Dell'acqua, R., & Eimer, M. (2008). Attentional capture by visual singletons is mediated by top-down task set: new evidence from the N2pc component. *Psychophysiology*, 45(6), 1013–1024.
- Kiss, M., Van Velzen, J., & Eimer, M. (2008). The n2pc component and its links to attention shifts and spatially selective visual processing. *Psychophysiology*, 45(2), 240–249.
- Lakatos, P., Shah, A. S., Knuth, K. H., Ulbert, I., Karmos, G., & Schroeder, C. E. (2005). An oscillatory hierarchy controlling neuronal excitability and stimulus processing in the auditory cortex. *Journal of Neurophysiology*, 94(3), 1904–1911.
- Leblanc, E., Prime, D. J., & Jolicoeur, P. (2008). Tracking the location of visuospatial attention in a contingent capture paradigm. *Journal of Cognitive Neuroscience*, 20(4), 657–671.
- Luck, S. J., Fan, S., & Hillyard, S. A. (1993). Attention-related modulation of sensory-evoked brain activity in a visual search task. *Journal of Cognitive Neuroscience*, 5(2), 188–195.
- Luck, S. J., Girelli, M., McDermott, M. T., & Ford, M. A. (1997). Bridging the gap between monkey neurophysiology and human perception: an ambiguity resolution theory of visual selective attention. *Cognitive Psychology*, 33, 64–87.
- Luck, S. J., Heinze, H. J., Mangun, G. R., & Hillyard, S. A. (1990). Visual event-related potentials index focused attention within bilateral stimulus arrays. II. Functional dissociation of p1 and n1 components. *Electroencephalography and Clinical Neurophysiology*, 75(6), 528–542.
- Luck, S. J., & Hillyard, S. A. (1990a). Electrophysiological evidence for parallel and serial processing during visual search. *Perception and Psychophysics*, 48(6), 603–617.
- Luck, S. J., & Hillyard, S. A. (1990b). Evidence for an ERP correlate of attentional filtering. *Society for Neuroscience Abstracts*, 16, 577.
- Luck, S. J., & Hillyard, S. A. (1994a). Electrophysiological correlates of feature analysis during visual search. *Psychophysiology*, 31(3), 291–308.
- Luck, S. J., & Hillyard, S. A. (1994b). Spatial filtering during visual search: evidence from human electrophysiology. *Journal of Experimental Psychology: Human Perception and Performance*, 20(5), 1000–1014.
- Mazza, V., Turatto, M., & Caramazza, A. (2009a). Attention selection, distractor suppression and n2pc. *Cortex*, 45(7), 879–890.
- Mazza, V., Turatto, M., & Caramazza, A. (2009b). An electrophysiological assessment of distractor suppression in visual search tasks. *Psychophysiology*, 46(4), 771–775.
- Mesulam, M. M. (1981). A cortical network for directed attention and unilateral neglect. *Annals of Neurology*, 10(4), 309–325.
- Oostenveld, R., Fries, P., Mairs, E., & Schoffelen, J. (2011). Fieldtrip: open source software for advanced analysis of MEG, EEG, and invasive electrophysiological data. *Computational Intelligence and Neuroscience*, 2011, 1–9.
- Posner, M. I., Walker, J. A., Friedrich, F. J., & Rafal, R. D. (1984). Effects of parietal injury on covert orienting of attention. *Journal of Neuroscience*, 4(7), 1863–1874.
- Robitaille, N., & Jolicoeur, P. (2006). Fundamental properties of the n2pc as an index of spatial attention: effects of masking. *Canadian Journal of Experimental Psychology*, 60(2), 101–111.
- Sauseng, P., Klimesch, W., Gruber, W. R., & Birbaumer, N. (2008). Cross-frequency phase synchronization: a brain mechanism of memory matching and attention. *NeuroImage*, 40, 308–317.
- Schack, B., Vath, N., Petsche, H., Geissler, H. G., & Moller, E. (2002). Phase-coupling of theta-gamma EEG rhythms during short-term memory processing. *International Journal of Psychophysiology*, 44, 143–163.
- Simson, R., Vaughn, H. G., Jr, & Ritter, W. (1977). The scalp topography of potentials in auditory and visual discrimination tasks. *Electroencephalography and Clinical Neurophysiology*, 42(4), 528–535.
- Tata, M. S., & Ward, L. M. (2005). Spatial attention modulates activity in a posterior “where” auditory pathway. *Neuropsychologia*, 43(4), 509–516.
- Telling, A. L., Kumar, S., Meyer, A. S., & Humphreys, G. W. (2010). Electrophysiological evidence of semantic interference in visual search. *Journal of Cognitive Neuroscience*, 22(10), 2212–2225.
- Treisman, A., & Souter, J. (1985). Search asymmetry: a diagnostic for preattentive processing of separable features. *Journal of Experimental Psychology: General*, 114(3), 285–310.
- Treisman, A. M., & Gelade, G. (1980). A feature-integration theory of attention. *Cognitive Psychology*, 12(1), 97–136.
- Wolfe, J. M., Cave, K. R., & Franzel, S. L. (1989). Guided search: an alternative to the feature integration model for visual search. *Journal of Experimental Psychology: Human Perception and Performance*, 15(3), 419–433.
- Woodman, G. F., & Luck, S. J. (1999). Electrophysiological measurement of rapid shifts of attention during visual search. *Nature*, 400(6747), 867–869.